

# Performance of *E. conferta* and *G. atroviridis* fruit extracts as sensitizers in dye-sensitized solar cells (DSSCs)

Hidayani Jaafar<sup>1,3</sup> · Mohd Fadzil Ain<sup>2</sup> · Zainal Arifin Ahmad<sup>1</sup>

Received: 6 March 2017 / Revised: 10 July 2017 / Accepted: 5 August 2017 / Published online: 11 August 2017  
© Springer-Verlag GmbH Germany 2017

**Abstract** Natural dyes extracted from *Eleiodoxa conferta* and *Garcinia atroviridis* were used for the first time as photosensitizers in dye-sensitized solar cells (DSSCs). Anthocyanin was identified as the main pigments that sensitize the semiconductor of TiO<sub>2</sub> film. Anthocyanin pigment contains hydroxyl and carboxylic groups in the molecule that can attach effectively to the surface of TiO<sub>2</sub> film. The optical characteristics of the extracted dye and photovoltaic performance of the cells were studied. The extracts showed UV–vis absorptions in the range of 530–560 nm with broad maxima absorption at ~430 nm. FTIR spectra of extraction revealed the presence of anchoring groups. For *E. conferta*, the photovoltaic performance of the sample with 3.16- $\mu\text{m}$ -thick TiO<sub>2</sub> produced the best results with open-circuit voltage ( $V_{\text{OC}}$ ), short-circuit current density ( $J_{\text{SC}}$ ), fill factor (FF), and energy conversion efficiency ( $\eta$ ) values of 0.37 V, 6.56 mA/cm<sup>2</sup>, 0.49, and 1.18%, respectively. The best photovoltaic performance for *G. atroviridis* was also obtained from the sample with 3.16- $\mu\text{m}$ -thick TiO<sub>2</sub> with  $V_{\text{OC}}$ ,  $J_{\text{SC}}$ , FF, and  $\eta$  values of 0.35 V, 3.74 mA/cm<sup>2</sup>, 0.65, and 0.85%, respectively.

**Keywords** Natural dyes · *E. conferta* · *G. atroviridis* · Dye-sensitized solar cell

✉ Zainal Arifin Ahmad  
srzainal@usm.my

<sup>1</sup> Structural Materials Niche Area, School of Materials and Minerals Resources Engineering, Universiti Sains Malaysia, Engineering Campus, 14300 Nibong Tebal, Penang, Malaysia

<sup>2</sup> School of Electrical and Electronic Engineering, Universiti Sains Malaysia, Engineering Campus, 14300 Nibong Tebal, Penang, Malaysia

<sup>3</sup> Faculty of Earth Science, Universiti Malaysia Kelantan, 17600 Jeli, Kelantan, Malaysia

## Introduction

Research on dye-sensitized solar cells (DSSCs) have drawn much attention in recent years, mainly due to their low manufacturing cost, easy fabrication, and relatively high-energy conversion efficiency ( $\eta$ ) [1, 2]. The DSSC consists of a metal oxide semiconductor as a photo anode, a dye sensitizer, an electrolyte, and a counter electrode [3]. In DSSC, the photo excitation of the dye sensitizer is followed by injection of electrons into the conduction band of the semiconductor. The dye molecule is self-regenerated by redox system at the counter electrode by electrons passing through the load [4]. The optimization of each component in DSSC is essential to achieve maximum efficiency.

In conventional DSSC, ruthenium (Ru) complex is the most efficient sensitizer for the sensitization of nanocrystalline TiO<sub>2</sub> semiconductor. However, the high cost and long-term unavailability of Ru complexes pushed many researchers to discover other cost-efficient sensitizers. The preparation of synthetic dyes also requires complicated procedures, organic solvent demands, and has low yield issues [5, 6]. Therefore, various investigations on easily available dyes extracted from natural sources that can be used as photosensitizers were conducted due to their large absorption coefficients, high light harvesting efficiency, low cost, easy preparation, and environmental friendliness [7–9]. The natural pigments are found in the shoot and root systems of plants such as flowers, leaves, fruits, stems, and roots. Several natural dye pigments, such as chlorophyll, betanins, carotenoids, anthocyanins, and tannins, are successfully used as sensitizers in DSSC application [10–12]. As reported by Wongcharee et al. [13], power conversion efficiency of DSSC using dyes extracted from blue pea, rosella, and mixture of both were 0.37, 0.05, and 0.15%, respectively. DSSC fabricated by dyes extracted from ivy gourd fruits and red

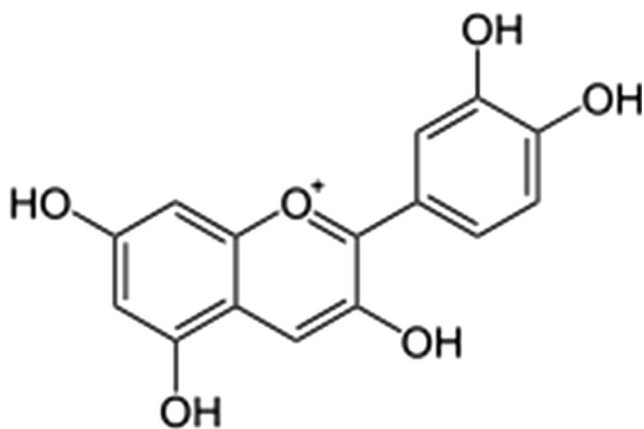


**Fig. 1** Structure of anthocyanin (cyaniding derivatives)

frangipani flowers were reported to reach an efficiency of 0.08 and 0.30%, respectively [12]. DSSCs fabricated using extracts from *Nerium oleander* (red pink), *Bougainvillea* (dark pink), and *Hibiscus* (red) were found to give conversion efficiency of 0.06, 0.05, and 0.19%, respectively [14]. Anthocyanins are the most important vascular pigments, belonging to the class of compounds named flavonoids [15]. The anthocyanins are responsible for the bright orange, pink, red, purple, and blue colors in some plant flowers and fruit, depending on the pH [16]. The hydroxyl and carbonyl groups present in the anthocyanin molecules [17] can be bound to the surface of porous  $\text{TiO}_2$  film, as shown in Fig. 1. This enhances the feasibility of electron transfer from the anthocyanin molecule to the conduction band of  $\text{TiO}_2$

[18]. To achieve higher efficiency, the natural dyes must bind strongly to the  $\text{TiO}_2$  surface by means of their anchoring group to ensure efficient electron injection into the conduction band of  $\text{TiO}_2$  [19]. The performance of natural dyes that contain anthocyanin pigment as sensitizers were evaluated by short-circuit current ( $J_{\text{SC}}$ ), open-circuit voltage ( $V_{\text{OC}}$ ), and energy conversion efficiency ( $\eta$ ) as is normally done by other researchers and is summarized as in Table 1.

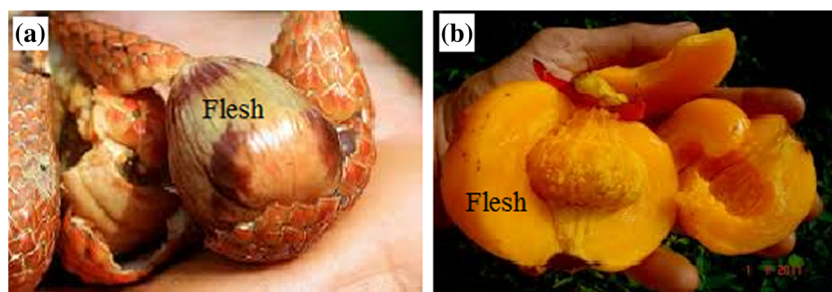
The performance of two types of tropical fruits, i.e., *Eleiodoxa conferta* and *Garcinia atroviridis* that are also known as *asam kelubi* and *asam gelugur*, respectively, in Malaysia, as sensitizers have never been reported. *E. conferta* contains oxalic, ascorbic, and malic acids [35]. It is reported that the highest concentration of oxalic acid ( $1.33 \text{ g/ml}^{-1}$ ) can be obtained from young fruits compared to mature stage ( $1.26 \text{ g ml}^{-1}$ ) and ripe stage ( $1.23 \text{ g ml}^{-1}$ ). Meanwhile, *G. atroviridis* fruit is containing citric, tartaric, malic, and ascorbic acids. Therefore, the selection of both *E. conferta* and *G. atroviridis* fruit is due to their raw natural dye extract that should perform better with the presence of natural extracts like organic acids and alcohols which behave as co-absorbate [23]. These suppress recombination of dye with electrolyte, favoring charge injection and reducing dye aggregation [36].

In this present work, *E. conferta* and *G. atroviridis* were extracted and used as a sensitizer for DSSC without further purification. The extracted dyes were characterized by ultraviolet–visible (UV–vis) and Fourier transform infrared (FTIR) spectroscopy. The photovoltaic performance ( $V_{\text{OC}}$ ,  $J_{\text{SC}}$ , FF,

**Table 1** Previous works on photovoltaic performance of natural dyes that contain anthocyanin pigment used in DSSC as sensitizers ( $\text{TiO}_2$  as photoanode)

Dye solution	Pigment used	$J_{\text{SC}}$ ( $\text{mA/cm}^2$ )	$V_{\text{OC}}$ (V)	$\eta$ (%)	Ref
<i>Rosa chinensis</i>	Anthocyanin	0.80	0.540	0.29	[20]
Black turtle beans	Anthocyanin	5.00	0.35	1.42	[21]
<i>Saraca asoca</i>	Anthocyanin	0.29	0.510	0.09	[22]
<i>Callindra haematocephata</i>	Anthocyanin	0.25	0.370	0.06	[23]
<i>Canarium odontophyllum</i>	Anthocyanin	9.74	0.35	1.43	[24]
<i>Begonia</i>	Anthocyanin	0.63	0.537	0.24	[25]
<i>Rhododendron</i>	Anthocyanin	1.61	0.585	0.57	[25]
Bauhinia tree	Anthocyanin	0.96	0.572	0.36	[25]
<i>Lithospermum</i>	Anthocyanin	0.14	0.337	0.03	[25]
Yellow rose	Anthocyanin	0.74	0.61	0.26	[25]
<i>Rosa xanthine</i>	Anthocyanin	0.64	0.49	-	[26]
<i>Hibiscus rosasinesis</i>	Anthocyanin	2.46	0.40	0.59	[27]
Pomegranate	Anthocyanin	12.20	0.39	2.00	[28]
Pomegranate	Anthocyanin	0.62	0.46	1.57	[29]
<i>Brassica olercea</i> (Redcabbage)	Anthocyanin	0.50	0.37	0.13	[30]
<i>Brassica olercea</i> (Redcabbage)	Anthocyanin	3.47	0.59	1.40	[31]
<i>Punica granatum</i> (Pomegranate)	Anthocyanin	2.05	0.56	0.59	[32]
<i>Lawsonia inermis</i> (Henna)	Anthocyanin	1.87	0.61	0.66	[33]
Black carrot ( <i>Daucus carota</i> L)	Anthocyanin	1.30	0.40	0.25	[34]

**Fig. 2** a *E. conferta* and b *G. atroviridis* fruits



and  $\eta$ ) of the fabricated DSSC was investigated using these extracts as sensitizers.

## Materials and methods

### Preparation of TiO<sub>2</sub> electrode

TiO<sub>2</sub> paste was prepared by blending 20 g of commercial TiO<sub>2</sub> nanocrystalline powder (Degussa P25) which was purchased from Sigma-Aldrich with 20 ml of ethanol and 3 ml of 0.1 M acetic acid until a thick paste was formed. Fluorine-doped tin oxide (FTO) conductive glass with a sheet resistance of  $\sim 7 \Omega/\text{cm}^2$  was cleaned in a detergent solution, rinsed using deionized water and ethanol, and then dried. The conductive site of the FTO conductive glass was identified using digital multimeter (All-Sun EM420B digital multimeter). TiO<sub>2</sub> films in thicknesses of 1.83, 3.16, and 7.60  $\mu\text{m}$  (as measured by FESEM) were obtained by taping 1-, 2-, and 3-layer thick adhesive tape, respectively, onto the conductive site in order to control the thickness. The TiO<sub>2</sub> paste was coated onto the FTO substrate using the doctor blade technique and sintered at 450 °C for 30 min.

### Preparation of natural dye sensitizers

The flesh of *E. conferta* and *G. atroviridis*, as shown in Fig. 2, were separated from the seeds and completely dried at room temperature. The flesh was crushed to powder form using a mortar. In total, 50 g of the powder was put into a beaker and added with 500 ml ethanol (1:10) and stirred. The mixture was left for 24 h in the dark at room temperature. The solid residues of the mixture were filtered out to obtain a pure and clear natural dye solution.

### Preparation of counter electrode

Carbon black was mixed with TiO<sub>2</sub> using the solid-state method as the counter electrode with weight ratio of 5:1 for TiO<sub>2</sub>/carbon black. The homogeneous carbon black paste was prepared by mixing the mixture (TiO<sub>2</sub>/carbon black) with 0.1 ml of Triton X-100 for 3 h. The conducting side of FTO glass was coated with 10 mM H<sub>2</sub>PtCl<sub>6</sub>

solution in ethanol, and the mixed paste was applied onto FTO glass using the doctor blade technique and sintered at 500 °C for 1 h.

### Assembly of DSSC

The TiO<sub>2</sub>-coated glass was obtained by immersing the films into the natural dye (*E. conferta* and *G. atroviridis*, respectively) for 24 h at room temperature. The sensitized electrodes were rinsed using ethanol to remove any unanchored dye. A drop of redox electrolyte (Iodolyte HI-30 with a concentration of 30 mM (Solaronix) and acetonitrile as solvent) was cast on the surface of sensitized photoanodes. The counter electrode was then clipped onto the top of TiO<sub>2</sub> working electrode with a cell active area of 6.5 cm<sup>2</sup> and then sealed using slurry tape.

### Cell characterization

UV–vis (HP 8453) was used to determine the absorption spectra of all samples. The FTIR spectra of dye extracts and dye-adsorbed TiO<sub>2</sub> films were measured using a Shimadzu FTIR spectrometer (IRAffinity-1) in the wave number range of 4000–500 cm<sup>-1</sup> with a maximum resolution of 0.5 cm<sup>-1</sup>. The thickness of the sample was observed using field emission scanning electron microscopes (FESEM) (Zeiss Supra 35VP). The photocurrent–voltage (I–V) curves of the DSSCs were recorded with a computer-controlled digital source meter (Keithley 2400) under an irradiation exposure of 100 mWcm<sup>-2</sup>.

## Results and discussion

### XRD analysis

Figure 3 shows the XRD patterns of the pure TiO<sub>2</sub>. The peaks indicate that the complete anatase structure (ICDD file no. 98-007-6028). The crystallite size was measured as per Scherrer's equation, where the average crystallite size of pure TiO<sub>2</sub> is 8.51 nm [37].

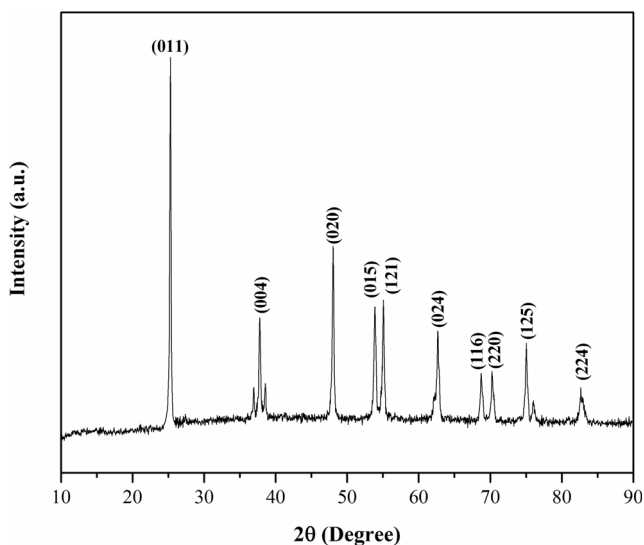


**Fig. 3** XRD patterns of pure TiO<sub>2</sub>

### FTIR spectra

The FTIR spectroscopy of pure and natural dye-sensitized TiO<sub>2</sub> nanoparticles is shown in Fig. 4. Both spectra have the characteristic vibration of Ti–O bond at 659 cm<sup>-1</sup> (in pure)

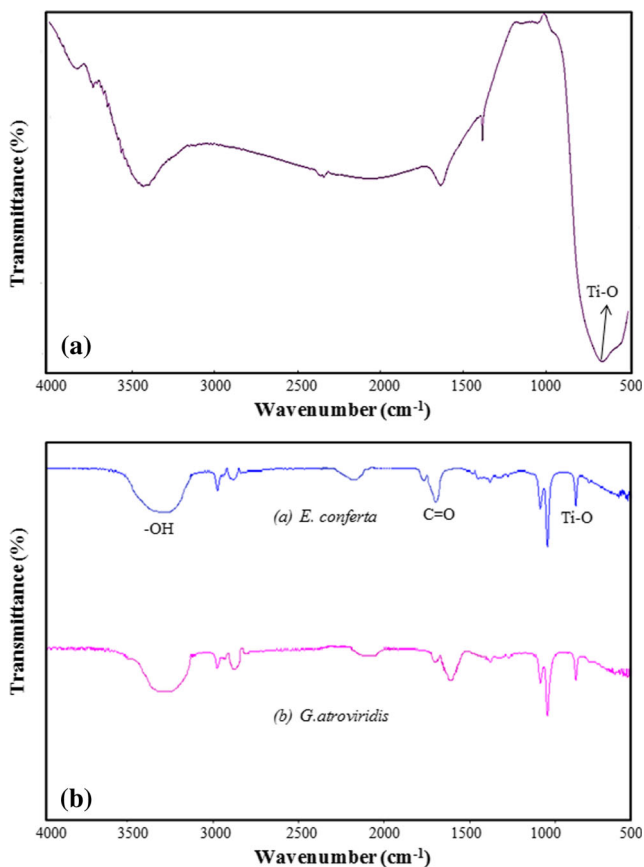
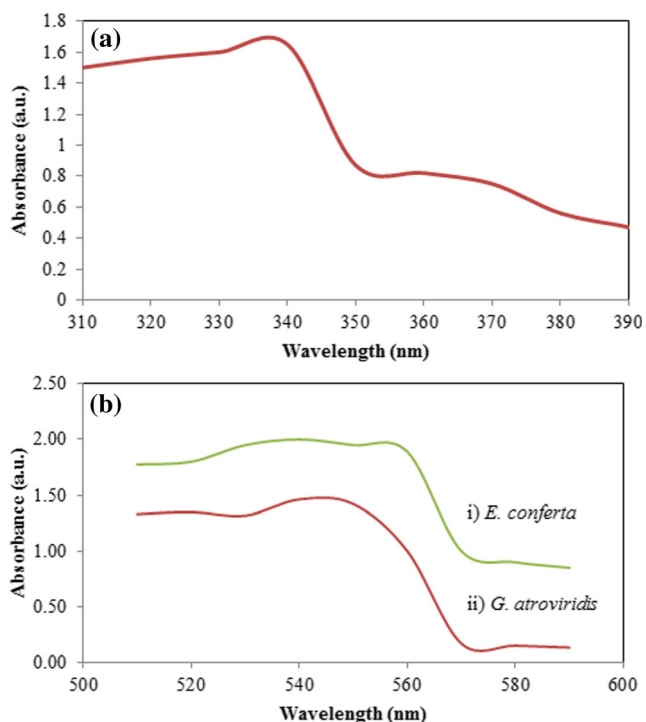


**Fig. 4** **a** Absorption spectrum of pure TiO<sub>2</sub> and **b** FTIR spectra of natural dye sensitized TiO<sub>2</sub> to indicate the presence of –OH, C=O, and Ti–O bonds

and 801 cm<sup>-1</sup> (in natural sensitizers) which normally occurs in between the standard range of 450–1000 cm<sup>-1</sup> [38]. The FTIR spectrums obtained from *E. conferta* and *G. atroviridis* are shown in Fig. 4b which demonstrates the presence of anthocyanin as all the characteristic peaks are matched to other similar research works [20, 23, 39]. The anthocyanin pigments were observed based on strong peak absorption in the range of 3000–3600 cm<sup>-1</sup> with wide and strong bands at 3336 and 3342 cm<sup>-1</sup> for *E. conferta* and *G. atroviridis*, respectively. The peaks correspond to the –OH stretching vibration for the anthocyanin dye of *E. conferta* and *G. atroviridis*. Both samples show peaks at 2974 and 2884 cm<sup>-1</sup> which corresponds to the –CH stretching modes that prove the presence of aromatic CH group. The broad absorption at 2078 cm<sup>-1</sup> indicates further electron delocalization into adjacent rings [13]. The C=O group stretching vibrations occur at 1741 cm<sup>-1</sup>. Since this group can also conjugate with ring double bonds, there is a strong stretching vibration at 1643 cm<sup>-1</sup> due to C=C aromatic ring stretching vibrations. The peaks at 1380 and 1381 cm<sup>-1</sup> for *E. conferta* and *G. atroviridis*, respectively, were assigned to the asymmetric –CH deformation modes of CH<sub>3</sub> group. The peaks at 1087 and 1046 cm<sup>-1</sup> could be attributed to C–O vibrations. Based on FTIR results, it is confirmed that the presence of hydroxyl (–OH) and carbonyl (C=O) groups in the molecular structure of anthocyanin dye can possibly bind with the surface of porous TiO<sub>2</sub> film. These bonds can be either monodentate or bidentate bridging. When illuminated, anthocyanin will absorb the light and electrons that are present when the HOMO state gets excited into the LUMO state. Therefore, electron injection takes place through the functional C=O and –OH groups into the conduction bands of TiO<sub>2</sub>.

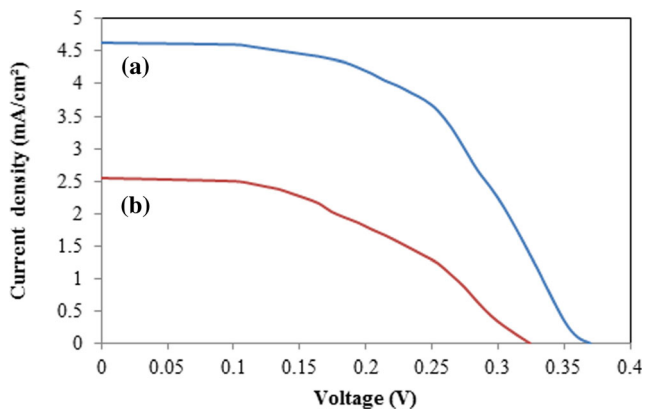
### UV–vis absorption

Figure 5 shows the absorption spectrum of pure TiO<sub>2</sub> and TiO<sub>2</sub> films adsorbed by (i) *E. conferta* and (ii) *G. atroviridis* dye solutions, respectively. The UV–vis absorption spectrum of pure TiO<sub>2</sub> nanoparticles shown in Fig. 5a indicated that the TiO<sub>2</sub> nanoparticles absorb light photons in UV and nearby regions only. Therefore, a separate dye sensitizer attached with TiO<sub>2</sub> is needed to ensure it is suitable for solar cell applications [40]. The absorption spectrum of natural dye-sensitized TiO<sub>2</sub> in Fig. 5b shows the enhancement of light photon absorption and extension of absorption region as compared to pure TiO<sub>2</sub>. The visible absorption band shifts to higher energy levels, showing a broad maximum around 530–560 nm with maximum absorption at 540 nm for *E. conferta*. Meanwhile, the absorption peaks were observed to be between 540 and 550 nm with maximum absorption at 540 nm for *G. atroviridis*. The spectrum obtained between 530 and 560 nm confirms the extraction of anthocyanin (cyaniding derivatives) [41]. Anthocyanin is



**Fig. 5** **a** Absorption spectrum of pure TiO<sub>2</sub>; **b** Absorption spectrum of natural dye sensitized TiO<sub>2</sub>

an important composition of some natural dyes and is often found in fruits, flowers, and leaves of plants. Due to its color which ranges from red to blue, it is prospected to become an efficient sensitizer for wide band gap semiconductors [39]. The broad absorption of *E. conferta* may result in absorption in photon energy at broader wavelengths which results in the generation of more photoelectrons [20]. The presence of hydroxyl and carbonyl groups in anthocyanin molecules allows it to easily bind with the surface of TiO<sub>2</sub> porous film; this is why it is suited for the application as sensitizers [42].



**Fig. 6** Current–voltage (*J*-*V*) characteristics of dye extracted from **a** *E. conferta* and **b** *G. atroviridis*

### Photovoltaic performance

Figure 6 shows the variation of the current–voltage (*J*-*V*) curve of *G. atroviridis* and *E. conferta*-based DSSCs, and Table 2 shows the performance of the natural dyes as sensitizers in DSSCs evaluated by *J*<sub>SC</sub>, *V*<sub>OC</sub>, FF, and *η*. *E. conferta* extracts produced promising photo electrochemical performance showing *J*<sub>SC</sub> = 4.63 mA/cm<sup>2</sup>, *V*<sub>OC</sub> = 0.37 V, FF = 0.56, and *η* = 1.00%. This is due to the presence of anthocyanin in the extract. With the help of anthocyanin, the extract sticks onto the oxide surface and increases its light harvesting ability. *G. atroviridis* extract has less efficiency values compared to *E. conferta* because of the low interaction between the extract and TiO<sub>2</sub> film. Based on Table 2, cells fabricated with *E. conferta* extract achieved highest power conversion efficiencies with maximum photocurrent, 4.63 mA/cm<sup>2</sup>. Natural extracts produced low *V*<sub>OC</sub> due to possible efficient electron/dye cation recombination pathways and the acidic dye adsorption environment [43]. The H<sup>+</sup> ions are potential determining ions for TiO<sub>2</sub>, and proton adsorption causes a positive shift of the Fermi level of the TiO<sub>2</sub>, thus limiting the maximum photovoltage that could be delivered by the cells.

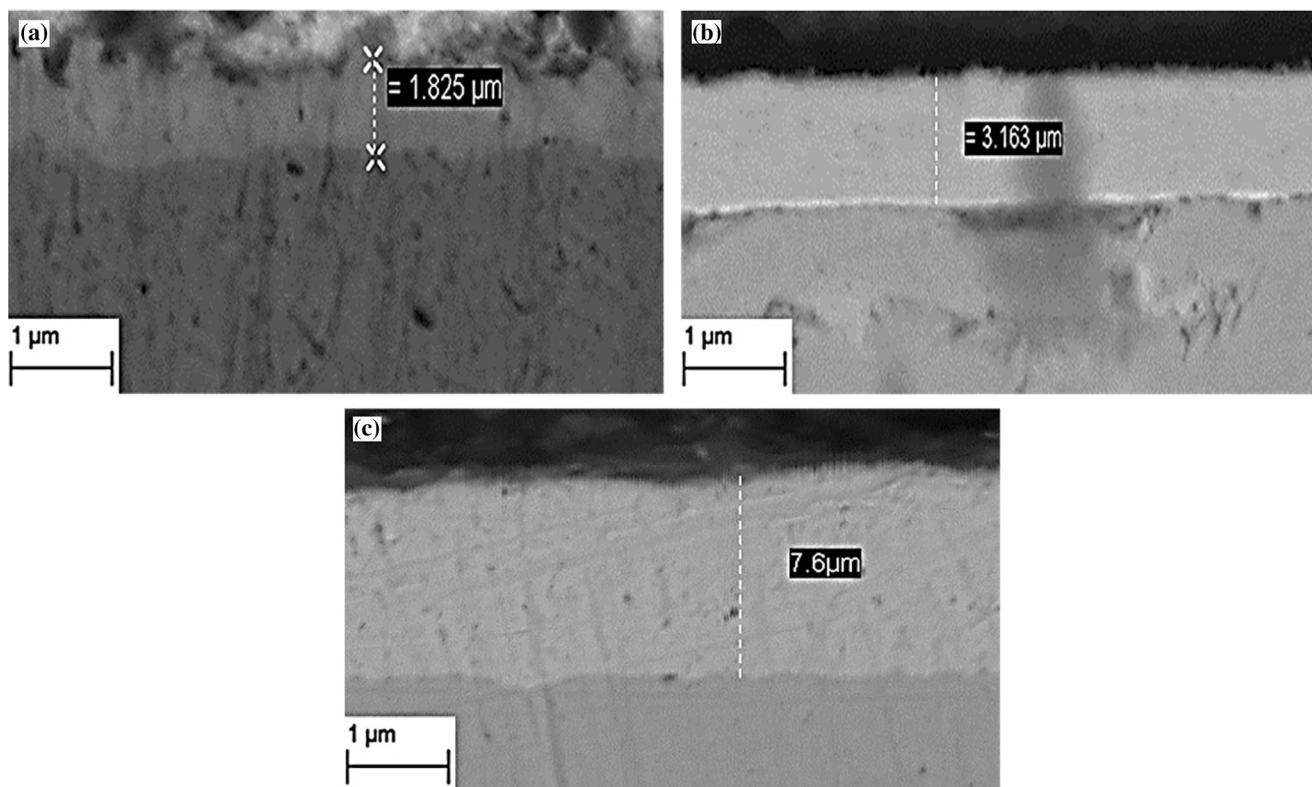
### Photovoltaic performance with different thicknesses of TiO<sub>2</sub> layers

Figure 7 shows FESEM images of the different thicknesses of TiO<sub>2</sub> layered onto FTO glass. In Fig. 6, 1.83 μm represents one layer of adhesive tape, 3.16 μm represents two layers of adhesive tape, and 7.60 μm represents three layers of adhesive tape. *E. conferta* and *G. atroviridis* used with the different thicknesses of TiO<sub>2</sub> layers indicated different photovoltaic performances, as shown in Figs. 8 and 9.

Figure 8 indicates that 3.16-μm-thick TiO<sub>2</sub> gave the highest result of 6.56 mA/cm<sup>2</sup> followed by TiO<sub>2</sub> 7.60 and 1.83 μm in thickness which gave results of 5.83 and 4.63 mA/cm<sup>2</sup>, respectively. In Fig. 9, the TiO<sub>2</sub> 3.16 μm in thickness also provides the highest result which is 3.74 mA/cm<sup>2</sup>, followed by the TiO<sub>2</sub> 1.83 μm and 7.60 μm in thickness which provided 2.55 and 1.82 mA/cm<sup>2</sup>, respectively. The photovoltaic performances of DSSC prepared with different thickness layers of TiO<sub>2</sub> are given in Tables 3 and 4 for *E. conferta* and *G. atroviridis*, respectively. Table 3 shows that the DSSC

**Table 2** Photovoltaic performances of DSSCs sensitized with *G. atroviridis* and *E. conferta*

Dye source	<i>J</i> <sub>SC</sub> (mA/cm <sup>2</sup> )	<i>V</i> <sub>OC</sub> /V	FF	<i>η</i> (%)
<i>G. atroviridis</i>	2.55	0.32	0.63	0.51
<i>E. conferta</i>	4.63	0.37	0.56	1.00



**Fig. 7** FESEM images of  $\text{TiO}_2$  in three different thicknesses on FTO glass **a** 1.83  $\mu\text{m}$  (1 layer of adhesive tape), **b** 3.16  $\mu\text{m}$  (2 layers of adhesive tape), and **c** 7.60  $\mu\text{m}$  (3 layers of adhesive tape)

sensitized with 3.16- $\mu\text{m}$ -thick  $\text{TiO}_2$  achieved  $V_{\text{OC}} = 0.37$  V,  $\text{FF} = 0.49$ , and  $\eta = 1.18\%$  which is higher compared to  $\text{TiO}_2$  1.83 and 7.60  $\mu\text{m}$  in thickness. Meanwhile, for Table 4, the DSSC using 3.16- $\mu\text{m}$ -thick  $\text{TiO}_2$  achieved  $V_{\text{OC}} = 0.35$  V,  $\text{FF} = 0.65$ , and  $\eta = 0.85\%$ . These results indicate that the efficiency of DSSC also depends on the thickness of  $\text{TiO}_2$  together with the types of sensitizers used. The enhancement in photocurrent with different thicknesses of  $\text{TiO}_2$  is due to the inherent energy barrier that leads to decrease in recombination of the electron [44].

The thickness of  $\text{TiO}_2$  affects the photovoltaic performance of DSSC because  $\text{TiO}_2$  is necessary in DSSC as it acts as an electron carrier after the electron was excited by the dye sensitizer when photon was absorbed. The increase in carrier amount as the thickness increases or when it reaches optimum thickness will increase the efficiency of the excitation-recombination process of the electrons which in turn results in increased output [45]. Generally, the DSSC efficiency performance that is dependent on  $\text{TiO}_2$  thickness is directly proportional to the increase in  $\text{TiO}_2$  layer, thereby leading to an

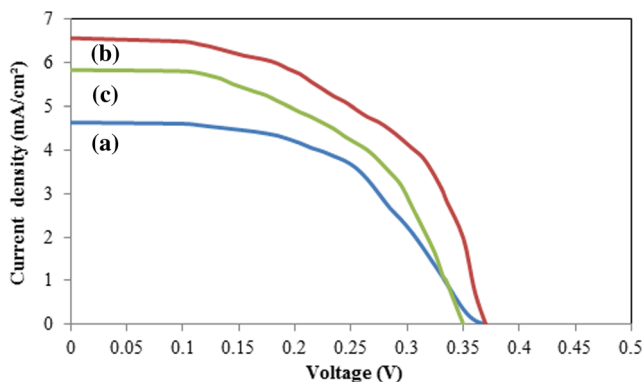


**Fig. 8** Comparison of current voltage ( $J$ - $V$ ) characterizations of *E. conferta* coated on different thicknesses of  $\text{TiO}_2$  layers: **a** 1.83  $\mu\text{m}$ , **b** 3.16  $\mu\text{m}$ , and **c** 7.60  $\mu\text{m}$

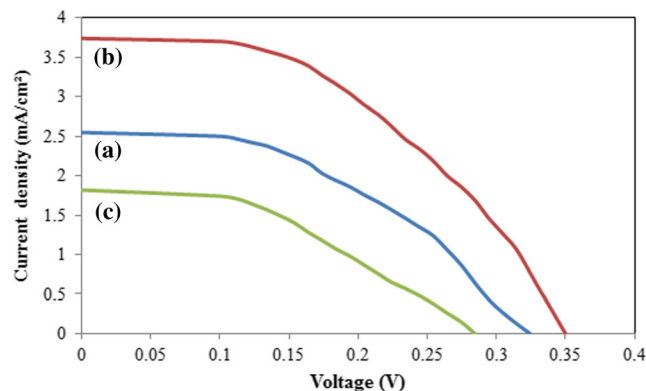


**Fig. 9** Comparison of current voltage ( $J$ - $V$ ) characterizations of *G. atrovirdis* coated on different thicknesses of  $\text{TiO}_2$  layers: **a** 1.83  $\mu\text{m}$ , **b** 3.16  $\mu\text{m}$ , and **c** 7.60  $\mu\text{m}$

**Table 3** Photovoltaic performances of *E. conferta* coated on different thicknesses of TiO<sub>2</sub> layers

Thickness of TiO <sub>2</sub>	J <sub>sc</sub> (mA/cm <sup>2</sup> )	V <sub>OC</sub> /V	FF	η (%)
1.83 μm	4.63	0.37	0.56	1.00
3.16 μm	6.56	0.37	0.49	1.18
7.60 μm	5.83	0.35	0.54	1.10

increase in absorbed photons which increases the amount of generated electrons [46]. Nevertheless, the increase in TiO<sub>2</sub> thickness increases the excitation-recombination process of electrons which may cause competition between rates of electron excitation and the recombination. Thus, this might help in determining the optimum thickness of TiO<sub>2</sub> for each extraction as the efficiency in DSSC performance begins to decrease.

#### Comparison of photovoltaic performances for 3.16-μm-thick TiO<sub>2</sub> layer

Table 5 presents photovoltaic DSSC parameters that were obtained from different dye extractions, *E. conferta* and *G. atroviridis*, and 3.16 μm thickness of TiO<sub>2</sub>. Their η are 1.18 and 0.85%, respectively. Extraction using *E. conferta* produced higher results compared to *G. atroviridis*; this is related to the anthocyanin bound to TiO<sub>2</sub> surface due to the reduction in undesirable contamination components in the dye matrix [47].

The η from natural dye extraction produces lower efficiencies compared to synthetic dyes (N719). This is due to the molecular structure of natural dye, the anchoring group in the natural dye (interaction dye with TiO<sub>2</sub>), and its stability. In natural dye, long chain structure with R groups such as xanthophylls hinders the bonding of the pigment with the oxide surface of TiO<sub>2</sub> [48]. Therefore, it prevents the dye molecules from becoming arrayed effectively on the TiO<sub>2</sub> film. Hence, there is a lack of electron transfer from the dye molecules to the conduction band of TiO<sub>2</sub> [49]. An improved efficiency using *E. conferta* is due to the presence of anthocyanin which helps to create a suitable bond on the surface of TiO<sub>2</sub>. In order to improve η, modification of photoanode and

**Table 4** Photovoltaic performances of *G. atroviridis* coated on different thicknesses of TiO<sub>2</sub> layers

Thickness of TiO <sub>2</sub>	J <sub>sc</sub> (mA/cm <sup>2</sup> )	V <sub>OC</sub> /V	FF	η (%)
1.83 μm	2.55	0.32	0.63	0.51
3.16 μm	3.74	0.35	0.65	0.85
7.60 μm	1.82	0.28	0.53	0.27

**Table 5** Photovoltaic performances of DSSCs of dye extracts at the optimum TiO<sub>2</sub> thickness

Dye extracts	TiO <sub>2</sub> thickness	J <sub>sc</sub> (mA/cm <sup>2</sup> )	V <sub>OC</sub> /V	FF	η (%)
<i>E. conferta</i>	3.16 μm	6.56	0.37	0.49	1.18
<i>G. atroviridis</i>	3.16 μm	3.74	0.35	0.65	0.85

counter electrode will help to improve the efficiency using natural dye extract.

## Conclusions

The extracts obtained from *E. conferta* and *G. atroviridis* were used as sensitizers in TiO<sub>2</sub> photoanode. The FTIR spectra of *E. conferta* and *G. atroviridis* confirmed the presence of –OH and C=O groups in the molecular structure of anthocyanin dye which means that it can be bound to the surface of porous TiO<sub>2</sub> film. The broad absorption of *E. conferta* may have resulted in absorption in photon energy at broader wavelengths, bringing about the generation of more photoelectrons, compared to *G. atroviridis*, affecting the photovoltaic performance. *E. conferta* indicated the highest photovoltaic performance compared to *G. atroviridis* using 3.16-μm-thick TiO<sub>2</sub> layer. *E. conferta* produced 1.18% of η with V<sub>OC</sub>, J<sub>SC</sub>, and FF values of 0.37 V, 6.56 mA/cm<sup>2</sup>, and 0.49, respectively.

**Acknowledgements** This research was supported by fundamental research grant scheme (FRGS) under grant number of 203/PBAHAN/6071263.

**Conflict of interest** No conflict of interest.

## References

1. Wang Y (2009) Recent research progress on polymer electrolytes for dye-sensitized solar cells. *Sol Energy Mater Sol Cells* 93:1167–1175. doi:10.1016/j.solmat.2009.01.009
2. Cheng X, Liang M, Sun S, Shi Y, Ma Z, Sun Z, Xue S (2012) Synthesis and photovoltaic properties of organic sensitizers containing electron-deficient and electron-rich fused thiophene for dye-sensitized solar cells. *Tetrahedron* 68:5375–5385. doi:10.1016/j.tet.2012.04.113
3. Kim HJ, Kim DE (2012) Effect of surface roughness of top cover layer on the efficiency of dye-sensitized solar cell. *Sol Energy* 86:2049–2055. doi:10.1016/j.solener.2012.04.007
4. Hao S, Wu J, Huang Y, Lin J (2006) Natural dyes as photosensitizers for dye-sensitized solar cell. *Sol Energy Mater Sol Cells* 80:209–214. doi:10.1016/j.solener.2005.05.009
5. Hamadian M, Safaei-Ghomi J, Hosseinpour M, Masoomi R, Jabbari V (2014) Uses of new natural dye photosensitizers in fabrication of high potential dye-sensitized solar cells (DSSCs). *Mater Sci Semicond Process* 27:733–739. doi:10.1016/j.mssp.2014.08.017

6. Isah KU, Ahmadu U, Idris A, Kimpa MI, Uno UE, Ndamitso MM, Alu N (2015) Betalain pigments as natural photosensitizers for dye-sensitized solar cells: the effect of dye pH on the photoelectric parameters. *Mater Renew Sustain Energy* 4:39. doi:10.1007/s40243-014-0039-0
7. Zhou H, Wu L, Gao Y, Ma T (2011) Dye-sensitized solar cell using 20 natural dyes as sensitizers. *Photochem Photobiol A Chem* 219:188–194. doi:10.1016/j.jphotochem.2011.02.008
8. Shahid M, Shahid-ul-Islam MF (2013) Recent advancements in natural dye applications: a review. *J Clean Prod* 53:310–331. doi:10.1016/j.jclepro.2013.03.031
9. Calogero G, Bartolotta A, DI Marco G, Di Carlo A, Bonaccorso F (2015) Vegetable-based dye-sensitized solar cells. *Chem Soc Rev* 44:3244–3294. doi:10.1039/c4cs00309h
10. Kay A, Gratzel M (1993) Artificial photosynthesis. 1. Photosensitization of titania solar cells with chlorophyll derivatives and related natural porphyrins. *J Phys Chem* 97:6272–6277. doi:10.1021/j100125a029
11. Calogero G, Yum JH, Sinopoli A, DI Marco G, Gratzel M (2021) Anthocyanins and betalains as light-harvesting pigments for dye-sensitized solar cells. *Sol Energy* 86:1563–1575. doi:10.1016/j.solener.2012.02.018
12. Shanmugam V, Manoharan S, Anandan S (2013) Performance of dye-sensitized solar cells fabricated with extracts from fruits of ivy gourd and flowers of red frangipani as sensitizers. *Spectrochim Acta Mol Biomol Spectrosc* 104:35–40. doi:10.1016/j.saa.2012.11.098
13. Wongcharee K, Meeyoo V, Chavadej S (2007) Dye-sensitized solar cell using natural dyes extracted from rosella and blue pea flowers. *Sol Energ Mat Sol Cells* 91:566–571. doi:10.1016/j.solmat.2006.11.005
14. Mary Rosana NT, Amamath JD, Vincent Joseph KL, Suresh A, Anandan S, Saritha G (2014) Natural sensitizers for dye sensitized solar cell applications. *Int J Chem Tech Res* 6:5022–5026
15. Szostak R, de Souza ECF, Antunes SRM, Borges CPF, Andrade A, Rodrigues P, Antunes A (2015) Anthocyanin from *Vitis labrusca* grape used as sensitizer in DSSC solar cells. *J Mater Sci Mater Electron* 26:2257–2262. doi:10.1007/s10854-015-2678-z
16. Raghvendra SV, Shakya A, Hedayetullah M, Arya GS, Mishra A, Grupta AD, Pachpute AP, Patel D (2011) Chemical and potential aspects of anthocyanins—a water-soluble vacuolar flavonoid pigments: a review. *Int J Pharm Sci Rev Res* 6:28–33
17. Sakata K, Saito N, Honda T (2006) Ab initio study of molecular structures and excited states in anthocyanidins. *Tetrahedron* 62:3721–3731. doi:10.1016/j.tet.2006.01.081
18. Calogero G, Citro I, DI Marco G, Minicante SA, Morabito M, Genovese G (2014) Brown seaweed pigment as a dye source for photoelectrochemical solar cells. *Spectrochim Acta A* 117:702–706. doi:10.1016/j.saa.2013.09.019
19. Ramamoorthy R, Radha N, Maheswari G (2016) Betalain and anthocyanin dye-sensitized solar cells. *J Appl Electrochem* 46:929–941. doi:10.1007/s10800-016-0974-9
20. Hemalatha KV, Karthick SN, Justin Raj C, Hong NY, Kim SK, Kim HJ (2012) Performance of *Kerria japonica* and *Rosa chinensis* flower dyes as sensitizers for dye sensitized solar cells. *Spectrochim Acta Mol Biomol Spectrosc* 96:305–309. doi:10.1016/j.saa.2012.05.027
21. Kimura Y, Maeda T, Iuchi S, Koga N, Murata Y, Wakamiya A, Yoshida K (2017) Characterization of dye-sensitized solar cells using five pure anthocyanidin 3-O-glucosides possessing different chromophores. *J Photochem Photobiol A Chem* 335:230–238. doi:10.1016/j.jphotochem.2016.12.005
22. Maurya IC, Neetu GAK (2016) Natural dye extracted from *Saraca asoca* flowers as sensitizer for TiO<sub>2</sub>-based dye-sensitized solar cell. *J Sol Energy Eng* 138:1–6. doi:10.1115/1.4034028
23. Maurya IC, Neetu, Gupta AK (2016) *Callindra haematocephata* and *Peltophorum pterocarpum* flowers as natural sensitizers for TiO<sub>2</sub> thin film based dye-sensitized solar cells. *Opt Mater* 60:270–276. doi:10.1016/j.optmat.2016.07.041
24. Lim A, Kumara NT, Tan AL, Mirza AH, Chandrakanthi RL, Petra MI, Ming LC, Senadeera GK, Ekanayake P (2015) Potential natural sensitizers extracted from the skin of *Canarium odontophyllum* fruits for dye-sensitized solar cells. *Spectrochim Acta A* 138:596–602. doi:10.1016/j.saa.2014.11.102
25. Zhou H, Wu L, Gao Y, Ma T (2011) Dye-sensitized solar cells using 20 natural dyes as sensitizers. *J Photochem Photobiol A* 219:188–194. doi:10.1016/j.jphotochem.2011.02.008
26. Hao S, Wu J, Huang Y, Lin J (2006) Natural dyes as photosensitizers for dye-sensitized solar cell. *Sol Energy* 80:209–214. doi:10.1016/j.solener.2005.05.009
27. Fernando JMRV, Senadeera GKR (2008) Natural anthocyanins as photosensitizers for dye-sensitized solar devices. *Curr Sci* 95:663–666
28. Ghann W, Kang H, Sheikh T, Yadav S, Chavez-Gil T, Nesbitt F, Uddin J (2017) Fabrication, optimization and characterization of natural dye sensitized solar cell. *Sci Rep* 7:41470. doi:10.1038/srep41470
29. Hosseinezhad M, Moradian S, Gharanjig K (2015) Fruit extract dyes as photosensitizers in solar cells. *Curr Sci* 109:954–956. doi:10.18520/v109/i5/953-956
30. Dumbra A, Georgescu A, Badea G, Enache I, Orrea C, Girtu MA (2008) Dye sensitized solar cells based on nanocrystalline TiO<sub>2</sub> and natural pigments. *J Optoelectron Adv Mater* 10:2996–3002
31. Chien CY, Hsu BD (2013) Optimization of the dye-sensitized solar cell with anthocyanin as photosensitizer. *Sol Energy* 98:203–211. doi:10.1016/j.solener.2013.09.035
32. Chang H, Lo YJ (2010) Pomegranate leaves and mulberry fruit as natural sensitizers for dye-sensitized solar cells. *Sol Energy* 84:1833–1837. doi:10.1016/j.solener.2010.07.009
33. Aduloju KA, Mohamed BS, Simiyu J (2011) Effect of extracting solvents on the stability and performances of dye-sensitized solar cell prepared using extract from *Lawsonia inermis*. *Fundam J Mod Phys* 1:261–268
34. Tekerek S, Kudret A, Alver U (2011) Dye-sensitized solar cells fabricated with black raspberry, black carrot and rosella juice. *Indian J Phys* 85:1469–1476. doi:10.1007/s12648-011-0166-8
35. Mokhtar SI, Aziz NA (2015) Organic acid content and antimicrobial properties of *Eleiodoxa conferta* extracts at different maturity stages. *J Trop Resour Sustain Sci* 3:72–76
36. Calogero G, DI Marco G, Cazzanti S, Caramori S, Argazzi R, Carlo AD, Bignozzi CA (2010) Efficient dye-sensitized solar cells using red turnip and purple wild Sicilian prickly pear fruits. *Int J Mol Sci* 11:254–267. doi:10.3390/ijms11010254
37. Jaafar H, Ahmad ZA, Ain MF (2017) Effect of Nb-doped TiO<sub>2</sub> photoanode using solid state method with *E. conferta* as sensitizer on the performance of dye sensitized solar cell. *Optik* 144:91–101. doi:10.1016/j.ijleo.2017.06.097
38. Li B, Wang X, Yan M, Li L (2002) Preparation and characterization of nano-TiO<sub>2</sub> powder. *MaterChemPhys* 78:184–188
39. Mozaffari SA, Saeidi M, Rahmanian R (2015) Photoelectric characterization of fabricated dye sensitized solar cell using dye extracted from red Siahkooti fruit as natural sensitizer. *Spectrochim Acta Mol Biomol Spectrosc* 142:226–231. doi:10.1016/j.saa.2015.02.003
40. Ananth S, Vivek P, Saravana Kumar G, Murugakoothan P (2015) Performance of *Caesalpinia sappan* heartwood extract as photo sensitizer for dye sensitized solar cells. *Spectrochim Acta Mol Biomol Spectrosc* 137:345–350. doi:10.1016/j.saa.2014.08.083
41. Harborne JB, Geissman TA (1956) Anthochlor pigments. XII. Maritimoin and marein. *J Am Chem Soc* 78:829–832



42. Tripathi M, Chawla P (2015) CeO<sub>2</sub>-TiO<sub>2</sub> photoanode for solid state natural dye-sensitized solar cell. *Ionics* 21:541–546. doi:[10.1007/s11581-014-1172-6](https://doi.org/10.1007/s11581-014-1172-6)
43. Su H, Huang YT, Chang YH (2015) The synthesis of Nb-doped TiO<sub>2</sub> nanoparticles for improved-performance dye sensitized solar cells. *Electrochim Acta* 182:230–237. doi:[10.1016/j.electacta.2015.09.072](https://doi.org/10.1016/j.electacta.2015.09.072)
44. Baglio V, Girolam M, Antonucci V (2011) Influence of TiO<sub>2</sub> film thickness on the electrochemical behaviour of dye-sensitized solar cells. *Int J Electrochem Sci* 6:3375–3384
45. D'Souza LP, Shwetharani R, Amoli V, Fernando CAN, Sinha AK, Balakrishna RG (2016) Photoexcitation of neodymium doped TiO<sub>2</sub> for improved performance in dye-sensitized solar cells. *Mater Des* 104:346–354. doi:[10.1016/j.matdes.2016.05.007](https://doi.org/10.1016/j.matdes.2016.05.007)
46. Fitra M, Daut I, Irwanto M (2013) Effect of TiO<sub>2</sub> thickness dye solar cell on charge generation. *Energy Procedia* 36:278–286. doi:[10.1016/j.egypro.2013.07.032](https://doi.org/10.1016/j.egypro.2013.07.032)
47. Singh LK, Karlo T, Pandey A (2014) Performance of fruit extract of *Melastoma malabathricum* L. as sensitizer in DSSCs. *Spectrochim Acta Mol Biomol Spectrosc* 118:938–943. doi:[10.1016/j.saa.2013.09.075](https://doi.org/10.1016/j.saa.2013.09.075)
48. Zhang D, Lanier SM, Downing JA (2008) Betalain, pigments for dye-sensitized solar cells. *J Photochem Photobiol A Chem* 195:72–80. doi:[10.1016/j.jphotochem.2007.07.038](https://doi.org/10.1016/j.jphotochem.2007.07.038)
49. Narayan MR (2012) Review: dye sensitized solar cells based on natural photosensitizers, renew. *Sustainable Energy Rev* 16:208–215. doi:[10.1016/j.rser.2011.07.148](https://doi.org/10.1016/j.rser.2011.07.148)